JOURNAL OF
ENVIRONMENTAL HYDROLOGY
The Electronic Journal of the International Association for Environmental Hydrology
On the World Wide Web at http://www.hydroweb.com
VOLUME 18 2010

GROUNDWATER MONITORING OPTIMIZATION IN INDUSTRIAL AREAS WITH UNKNOWN EMISSIONS

Luís Miguel Nunes | Faculty of Sciences and Technology
University of Algarve
Faro, Portugal

A solution is proposed to the problem of finding the best monitoring network design for the detection of groundwater contamination from multiple areal sources with different leakage probabilities and amounts leaked. In large industrial plants or industrial areas the probability of occurrence, and the amount of contaminant released in a leak varies from place to place, which, in turn, makes the contamination plume spatial distribution stochastic. One way to model this randomness is by simulating the sources as random (models the cause); others include the Monte Carlo simulations of permeability and/or dispersivity fields (models the effect). In the method proposed here flow and transport modeling are coupled with the random simulation of the sources, followed by measuring the accuracy and precision of several candidate monitoring network designs by way of a specific objective function. As the selection of the locations is a very difficult combinatorial problem, a simulated annealing algorithm is proposed for the optimization. The method was applied to a hypothetical case study consisting of an unconfined porous aquifer with risk of contamination from an industrial area. Results show that the method proposed is highly preferable to stratified and clustered monitoring.

INTRODUCTION

Groundwater pollutants may originate from point or non-point sources. A point source is characterized by having identifiable, small to very small scale sources. Non-point sources are usually associated with diffuse/spread contamination, eventually originated from many small-scale sources. Most common point-sources for groundwater are leaking underground storage tanks (USTs), septic systems, landfills and hazardous wastes sites. Most common non-point sources include agriculture, road runoff, and leaks or spills of industrial chemicals at industrial sites. In the United States, between 1988 and 2006, 464,728 releases from leaking USTs were confirmed (data available in the MRP*Info database: USEPA (2006)). The yearly frequency of a leak given an accident at an industrial site in the USA, for the 1994-1999 period, with data from Belke (2000), was calculated as 0.1119, as opposed to a value of 0.3182 for UST leakage frequency. Using the same data on can calculate, using Bayes theory, the probability of having an accident in the origin of a leak, equal to 0.0820, and the probability of detecting a leak if no accident has occurred, which amounts to 0.02987. Note here that the probability of having a leak in a UST (@ 32%) is much higher than that reported for industrial releases (@ 11%), indicating that USTs alone are very important contamination sources. In the European Union, as far as it was possible to investigate, there is no global quantification of UST releases, however, the estimated number of contaminated sites exceeds 1.5 million as this number is from only 11 of 25 member states (EEA, 1999). USTs are not, however, the only sources in industrial areas. Accidental spills are also common, e.g., when transferring chemicals between tanks. Chemical releases may also be due to ruptures in piping systems, and in welding points. Pipe rupture leakage frequency or rupture frequency may be determined by the well-known "Thomas methodology" (Thomas, 1981), if no historical data or specific maintenance records are available. It must be used with care as it may not have sufficient discriminating power about piping reliability (Lydell, 2000). The Thomas approach is only an alternative method whenever historical information is not available; otherwise probabilistic analysis of accidents and incidents kept in databases is advised. Examples of such databases include MHIDAS (Major Hazard Incident Data Service), developed by the Safety and Reliability Directorate of the United Kingdom Atomic Energy Authority, the FACT (Failure and Accident Technical Information System) operated by the TNO (Organization for Applied and Scientific Research) in Holland; and the RMP*Info (Risk Management Plans Database) operated by the United States Environmental Protection Agency. Once a contaminant enters groundwater it will spread and interact with the soil matrix. Spreading is mainly in the direction of groundwater flow, with spreading velocities that may be faster, equal or slower (i.e., "retarded" - used here in the same sense as in Zheng (1990)) than that of the groundwater itself. In the first case are light non-aqueous phase liquids that in some particular conditions may spread on the top of the groundwater table faster than the water itself, and eventually in different directions (Mercer and Cohen, 1990); Newell et al., 1995)). Retarded contaminants interact with the soil matrix, by sorption and strong chemical bonds. All cations and many organic molecules undergo retardation in soil, with the strength of the sorption dependent on the chemical characteristics of the contaminant and on the amount of available sorption "sites" (depending on the amount and type of clay, organic matter, metal oxides and hydroxides). Accurate prediction of contaminant spreading is fundamental to the correct allocation of monitoring devices and design of treatment techniques. Quantitative prediction of contaminant spreading is only possible if one understands the processes controlling advection, dispersion and reaction (physical, chemical, biological) and affecting concentrations. These processes may be incorporated in models, thus helping to model complex

time and space processes. Uncertainty about parameters may also be incorporated in modeling, resulting in stochastic predictions of groundwater concentrations. Uncertainty is usually related to incomplete information about hydraulic parameters (hydraulic conductivity at the top of the list), dispersion parameters (mostly dispersivity), reaction parameters (usually the distribution coefficient between solute and solid phases, biological reaction constants and rates, and radioactive decay), and source location and amounts released.

Uncertainty about receptor concentration values given some emission is a result of some factors that may act synergistically, of which the most important are uncertainty about: i) the permeability field; ii) the flow boundary conditions; iii) the dispersivity coefficients; iv) the initial conditions; v) uncertainty about mass boundary conditions (amounts emitted by the source(s)). The first three factors have been studied exhaustively for the last thirty years (see, e.g., the review made by ASCE (2003)), though a thorough review pointing specific rules and conditions of application is still missing. The latter two factors have been the subject of a broad set of methods included under the designation of "chemical fingerprinting". Though these methods were usually aimed at identifying compounds responsible for contamination, using laboratory analytical methods, they have also been important in environmental forensics to identify the contamination sources in groundwater, namely of petroleum hydrocarbons (Zemo et al., 1995; Stout et al., 1998), persistent organics (Erickson, 1997; Ramamoorthy and Ramamoorthy, 1997), agriculture contamination with specific nutrients (Widory et al., 2004), proprietary additives and other chemicals (Atmadja and Bagtzoglou, 2001; Morrison, 2000a,b). In some instances fingerprinting is not sufficient to attribute responsibilities beyond a reasonable doubt (Stout et al., 1998). In most cases also releases and spill history (location and amounts spilled), chemical parent products and historical records are necessary. Furthermore, by accurately identifying pollution sources, the complex and lengthy process of remediation that is often initiated by finding the contamination source can be cut down (Abt, 1999). Furthermore, contaminant source uncertainty is one of the factors causing the problem to be ill-posed when solving contaminant transport problems, meaning that a small perturbation in the input may result in an arbitrary large perturbation in the solution (Sun, 1994). Perturbations in contaminant source can be caused by limitations in data quantity and quality, and by model uncertainty, which may be non-Gaussian and systematic (Sun et al., 2006). Common model uncertainties include parameter uncertainty and model structure uncertainty. The former may be caused by the variability of hydrogeologic parameters manifested at different spatial scales, whereas the latter is due to incomplete knowledge or incorrect conceptualization of system features, events, and processes (Meyer et al., 2004).

The most common approach to include uncertainty in modeling is by stochastic modeling. Here, hydraulic conductivity, K, is considered a random field and a large number of flow and transport simulations are made (e.g., by Monte Carlo simulation, either conditioned on some known values, or not) with alternative simulated K values (Kaunas and Haimes, 1985; Massmann and Freeze, 1987; Massmann and Freeze, 1987b; Small, 1997) and extracting the relevant information from the results, such as classical statistical parameters and frequency analysis (e.g., by entropy) and Bayesian posterior distributions, necessary to evaluate the objective functions. Meyer et al. (1994), Storck et al. (1997) and Hudak (2005) also consider the shape and probability of release at the source – though the releases are modeled by uniform distributions, either at the border of the emitting area (landfill) or inside it, with no constraint as to where inside the area the release occurs. Reinelt et al. (1988) proposed a computer-aided methodology to aid implementing a monitoring program at the watershed level, with uncertainty about source and sinks, where human

activities resulted in non-point contamination sources. They developed an algorithm (design) to examine tradeoffs between cost and statistical power for the stations where detection of change was the primary objective. One interesting result from this study is that, in the case study evaluated - Stillaguamish river basin - it was more cost-effective to increase the number of stations than to increase sampling frequency or number of replicates. For detection monitoring this may well be the most frequent situation - increasing frequency or replicates at wrongly situated stations will not result in important power increase, when compared to the gain obtained by putting a station at a better location. Scheibe and Lettenmaier (1989) use a health risk-based methodology, where the probability of detecting contamination at a given monitoring well depends on the probability of having applied the contaminant in some upstream soil plots in agricultural areas. The objective was to minimize added health risk for the selected observation monitoring wells. The method proposes an iterative procedure of sampling-analysis-sampling, where many health risk parameters have to be (professionally) assumed.

In the present article, instead of making the permeability field the cause for the uncertainty at monitoring wells, the uncertain parameter is contaminant release location and amount released. The probability of a leak and the amount of contaminant released are modeled as random functions with known mean and standard deviation. Information regarding these two parameters may be obtained for some industries and processes in specific databases, as mentioned earlier. Several Monte Carlo simulations are then conducted to obtain alternative emission scenarios. Two-dimensional flow and transport simulation is made using these scenarios, resulting in as many alternative plume concentration distributions. An optimized monitoring network is then sought with the highest reliability (accuracy and precision), i.e., that best quantifies i) the spatial variability of concentrations; ii) contaminated area and volume. Optimization is made by the simulated annealing algorithm due to the combinatorial nature of the problem of selecting a small number of well locations from a large set of alternatives. The optimized network is then compared to other common statistical methods: clustered and stratified. The latter were chosen as they are the most frequently used: clustered when monitoring is concentrated near the origin due to legal constraints (e.g., property limits and drilling permits) or empirical decision; stratified when the latter is extended to outer limits, but more information is considered necessary near the origin. Results show that optimization generated monitoring networks outperform these configurations.

The article is organized as follows: in the second section some methods are reviewed, namely for i) obtaining the emission scenarios, ii) groundwater flow and solute transport, iii) objective function formulation; iv) solving the optimization problem; the third section presents a case study; in the fourth section the results are analyzed and compared; finally, in the last section the main conclusions are drawn.

METHODOLOGY

Estimating leakage probability and mass flux at the source

Leakage events are more frequent in certain industrial activities and processes (sources) than in others; likewise the amount of contaminants released also varies in space. Hence, a method for estimating contamination events must take these two aspects into consideration. Here, the likelihood of a leak is modeled by a leakage probability attributed to sub-areas inside the industrial area, where specific activities or processes take place, and the amount released is modeled by setting the confidence interval to the mean contaminant concentration, meaning that the leakage

concentration may vary in between two pre-established values. Variability of the source was created by a very simple algorithm intended to generate several alternative, equally probable, leakage scenarios, in a number of, say, k. A grid was superposed over the industrial area, and each grid cell receives its own emission parameters. The probability of a leak occurring at grid cell i is given by p_i, and the *potential emission* concentration (M/L^3) is given by c_i, such that c_i is a value in the interval $[m_i-\delta_i.m_i,\ m_i+\delta_i.m_i]$, with m_i the *mean potential emission* value and δ_i the interval amplitude (M/L^3) for some confidence level. The δ_i parameters could also be established by fuzzy logic, in which case the parameter may take different values to the left and right of the central value, or by professional judgment based on previous experiences or similar cases. To estimate *effective emission* concentration, e_i, a random number, r_i, is drawn from an uniform distribution, and the following simple pseudo-code is used: i) if $p_i > r_i$ then $\pi_i = 1$; else $\pi_i = 0$; ii) randomly obtain the *potential emission* concentration, c_i, inside the interval $[m_i-\delta_i.m_i,\ m_i+\delta_i.m_i]$; iii) calculate the *effective emission* by $e_i = c_i\ .\ \pi_i$; iv) go to i) until all cells have been calculated; repeat i) to iv) k times (see Equation (3) and accompanying text).

Estimating cell concentrations

Contaminant concentration estimates are obtained by solving the advection-dispersion differential equations for mass transport in porous media with the appropriate state variables and initial and boundary conditions. Considering that a two dimensional model of steady-state saturated groundwater flow in an isotropic heterogeneous aquifer is applied on a rectangular domain of dimension ($0 \le x \le L_x$, $0 \le y \le L_y$), the equation to be solved is

$$\frac{\partial}{\partial x}\left(K_{xx} \frac{\partial h}{\partial x} \right) + \frac{\partial}{\partial y}\left(K_{yy} \frac{\partial h}{\partial y} \right) = 0 \tag{1}$$

where Kxx is the hydraulic conductivity in the x direction [L/T], Kyy is the hydraulic conductivity in the y direction [L/T] and h is the hydraulic head[L]. If the contaminant is assumed to be conservative, with no interaction with the solid matrix, then the two-dimensional advection-dispersion equation for plume migrating in a flow domain is (Bear, 1972):

$$v_x \frac{\partial C}{\partial x} + v_y \frac{\partial C}{\partial y} - D_{xx} \frac{\partial^2 C}{\partial x^2} - D_{yy} \frac{\partial^2 C}{\partial x^2} = \frac{\partial C}{\partial t} \tag{2}$$

where C is the concentration of the contaminant in cell at location (x, y), v_x and v_y are the average groundwater flow velocity components in the x and y direction respectively, D_{xx}, D_{yy} are the components of the pore scale hydrodynamic dispersion vector, and t is time. Out of the many numerical solvers for these equations, either freeware or in commercial versions, the most appropriate ones for automatic generation of receptor concentration scenarios are those that allow a direct access to input and output files and that may run as slaves of other programs. MODFLOW (McDonald and Harbaugh, 1988) for flow modeling and MT3D (Zheng, 1990) for advection-dispersion-chemical reaction modeling are examples of such codes, and were used here. In order to obtain a representative image of the contamination phenomenon under uncertainty about the source presented in the previous section, several estimates of concentration are needed. If one considers the variance of the *effective emission*, e, represented here as s_e^2, a threshold value d, representing the error one is willing to accept when estimating the mean value of e, for a two-sided confidence level, α, Equation (3) may help determine the number of alternative scenarios needed to have a representative sample. The dimension of the representative sample is therefore

associated with the variability at the source and not with the variability of the estimated concentration fields because only the mass flux at the sources is considered stochastic, i.e., flow and transport are modeled deterministically.

$$k = \frac{1}{\frac{d^2}{z^2 s_e^2} + \frac{1}{P}} \tag{3}$$

In Equation (3) k stands for the number of alternative scenarios, z denotes the upper $\alpha/2$ point of the standard normal distribution, and P is the number of original samples (proposed here to be the number of cells inside the emission area), such that $P >> \frac{z^2 s^2}{d^2}$.

Optimizing the monitoring network

The optimization problem is stated as: find the locations for installing monitoring wells that guarantee the highest reliability (accuracy and precision), i.e., that best quantify i) the spatial variability of concentrations; ii) contaminated area and volume. Accuracy is measured as the kriging variance (variance of the estimation errors) and precision as the mean absolute error calculated between the concentration estimates obtained with the entire population and those obtained with a sample from that population. Kriging is a well-known estimation method that looks for maximum accuracy. When estimating a variable in discretized spatial field (e.g., grid) with kriging the following information will be obtained at each grid node (or grid area): i) the estimated value; ii) variance of the estimation error (kriging variance). As will be seen below, the latter is independent of the actual value of the variable at the grid node, being instead dependent on the spatial distribution of the original data used in the estimation. This feature makes it possible to alter the location of original data locations and evaluate its effect in the estimated accuracy. Consider as the population all the central nodes of the cells in the conceptual model used to estimate the receptor concentrations (of very large size, say, N). Consider also that all these nodes are alternative locations to install monitoring wells (the sample). As it is impractical and unnecessary to monitor in all locations (entire population) some of them will have to be chosen (both sample size, n, such that $n < N$, and their location). This result is a combinatorial problem with a solution space of size equal to the number of possible combinations when extracting n elements from a population of size N., which attain very large numbers even for small n and N. Testing exhaustively all solutions is therefore impossible for most practical cases. Problems of this combinatorial nature are usually very hard to solve, and no solution may be attained in polynomial time (calculation time grows with the dimension of the problem (combinations) faster than any polynomial function). Some alternative optimization algorithms have been proposed to obtain a solution (a minimum or a maximum), but in most cases there is no guarantee that the solution is optimal (the minimum of the minima, or maximum of the maxima). The most successful algorithms proposed to solve such problems are the metaheuristics Simulated Annealing (SA), Tabu Search (TS), Genetic Algorithms (GA), Ant Colonies (AC), other nature-based algorithms (e.g., Sworm Intelligence), combinations of these with each other, and combinations with more classical methods such as branch-and-bound (-cut), linear programming, and gradient methods. Of these the only with demonstrated convergence to the optimal value is SA, but this will, unfortunately, only happen for very large processing times (very large Markov chains) (Aarts and Korst, 1990;

Laarhoven and Aarts, 1987). SA has also been demonstrated to be a very powerful algorithm to solve positioning problems (Nunes et al., 2004). In the following a more thorough discussion is presented of both the kriging estimation method and the simulated annealing optimization algorithm, before presenting the objective function.

Kriging

The values of a variable at the sampled points in the field can be considered as realizations of a set of random variables in a field Γ. A set of random variables defined in a field Γ is a random function. The most common theory considers that the random function is invariant under translation. Strictly, the restrictive hypotheses are applied only to the first two moments, hence they are only required to exist and be independent of space coordinates (second order stationarity), or the spatial covariance of the variable should be dependent only on the distance h between two coordinates. In this case only the spatial increments have to be stationary (intrinsic stationarity). If these increments are made at step h, then the resulting expression is called the variogram. A linear estimation of concentration, C can be obtained from p data points by

$$C = \sum_{i=1}^{p} \kappa_i \cdot C(x_i) \tag{4}$$

which is unbiased if the sum of the weights κ_i is one. This is a common requirement in several estimation methods, and also in kriging. The estimation variance (kriging variance) is expressed by (Journel and Huijbregts, 1978),

$$\sigma_E^2(A) = \sum_{i=1}^{n_A} \kappa_i \cdot \gamma(h_{iA}) - \gamma(h_{AA}) + \mu \tag{5}$$

with $\gamma(h_{iA})$ the average variogram between locations with known concentration and the cell to be estimated, A; $\gamma(h_{AA})$ is the average variogram inside the cell; m is the Lagrange parameter; κ_i are kriging weights. The estimation variance is a measure of the estimation accuracy of C. Because $\sigma_E^2(A)$ only depends on the geometric configuration of the data points, once a variogram model is defined, it is possible to change data locations and calculate the estimation variance again. The spatial arrangement of points that minimizes $\sigma_E^2(A)$ has the lowest estimation variance, and this therefore best reflects the spatial correlation introduced in the variogram model. As the estimation variance is a local measure of accuracy (at A), a global measure is needed to allow the comparison of two alternative spatial configurations. Woldt and Bogardi (1992) proposed an average measure of estimation variance weighted by prior suspicion of the value C, and the average measure of kriged contamination level weighted by estimation variance as the global measure. Here an analogous measure is used, but considering equal weights, i.e., a simple mean of the estimation variance,

$$\sigma_E^2 = \frac{1}{N} \sum_{i=1}^{N} \sigma_E^2(A_i) \tag{6}$$

where A_i denotes each of the cells to be estimated, and N is the number of model cells to be estimated. The cells are then identified by N points (e.g., their central points). Equation (6) reflects the accuracy of estimating with a set of stations, and the more accurate the estimates, the lower the mean estimation variance. Therefore, a set of stations with a spatial configuration that will

generate an estimated field with lower mean estimation variance will be preferred to another set with a higher variance.

Simulated annealing

Simulated annealing is classified as a metaheuristic algorithm, devised as a top-level general strategy which guides other heuristics to search for feasible solutions in domains where the task is hard. Metaheuristics have been most generally applied to problems classified as NP-Hard or NP-Complete by the theory of computational complexity. However, metaheuristics can also be applied to other combinatorial optimization problems for which it is known that a polynomial-time solution exists but is not practical. They can be seen as a general algorithmic framework which can be applied to different optimization problems with relatively few modifications to make them adapted to a specific problem. Other examples of metaheuristics are Tabu Search, Genetic Algorithms and Mimetic Algorithms. Simulated Annealing (SA) is an analogy between the way in which a metal cools and stabilizes into a minimum energy crystalline structure (designated in metallurgy as the annealing process) and the search for a minimum in a more general system. The algorithm is based upon that of Metropolis et al. (1953), which was originally proposed to find the equilibrium configuration of a collection of atoms at a given temperature. The connection between this algorithm and mathematical minimization was first proposed by Kirkpatrick et al. (1983) and Cerny (1985) who proposed that it form the basis of an optimization technique for combinatorial (and other) problems. SA's major advantage over other methods is an ability to avoid becoming trapped at local minima. The algorithm employs a random search which not only accepts changes that decrease objective function, but also some changes that increase it. The latter are accepted with a, usually decreasing, probability as the annealing process evolves. The Metropolis criterion is as follows: consider that the change in the objective function is $\Delta\sigma_E^2$; if $\Delta\sigma_E^2 \leq 0$, then the change in the system is accepted and the new spatial configuration is used as the starting point in the next step; if $\Delta\sigma_E^2 > 0$ then the probability that the change is accepted is determined by $P(\Delta\sigma_E^2) = exp(-\Delta\sigma_E^2/t)$, where t is a control parameter called temperature; a random number uniformly distributed in the interval (0,1) is taken and compared with the former probability; if this number is lower than $P(\Delta\sigma_E^2)$ then the change is accepted. The SA algorithm runs as follows: i) the system is *melted* at a high temperature (initial temperature, t_1); ii) the temperature is decreased gradually until the system *freezes* (because no better solutions are found and the probability of uphill steps is near zero); iii) at each iteration the Metropolis procedure is applied; iv) if any of the stopping criteria are reached the algorithm is stopped and the best solution found is presented. The generic SA algorithm for a minimization, considering a neighborhood structure χ , and an objective function σ_E^2 has the following pseudo-code:

Select an initial solution X_{best};

Select an initial temperature $t_1>0$;

Select a temperature reduction factor, η;

Repeat

  Repeat

    Randomly select $X \in \chi\ (X_{best})$;

    $\Delta\sigma_E^2 = \sigma_E^2\ (X) - \sigma_E^2\ (X_{best})$;

if $\Delta\sigma_E^2 \leq 0$ then

$X_{best} = X$

otherwise

generate random θ uniformly in (0,1);

if $\theta < \exp(-\Delta\sigma_E^2/t)$ then $X_{best} = X$;

Until *iterations* = *max_iterations*

Set $t = \eta\, t$;

Until stopping conditions = true;

X_{best} is the optimal solution found.

Several improvements have been proposed to speed up the process, namely, by limiting the dimension of the Markov chain (*max_iterations*) and the number of successful solutions (*max_best*) at each temperature, whichever comes first. If the average value of the OF does not change after a pre-established number of temperature decreases, then the annealing may also be stopped. These parameters control the time spent at each temperature and the total running time. Along with these dynamic criteria, a static one may be used to halt the process when a minimum temperature, is reached. This will guarantee that the annealing stops if none of the dynamic criteria are fulfilled, even before the total number of iterations is attained. In our algorithm both the dynamic and the static criteria were implemented. The initial temperature, t_1, is calculated by running a fast (rapid temperature decrease) schedule and picking up the temperature for which more than 95% of the iterations are accepted. Temperature is usually decreased at a constant rate, η, usually close to one (e.g., 0.90 or higher). Aarts and Korst (1990) showed that SA can find optimal solutions if equilibrium is attained at each temperature (constant objective function mean and variance) and proposed a temperature schedule dependent on the objective function variance to guarantee that outcome. Despite this very attractive characteristic, such a schedule tends to converge too slowly. Other t schedules for optimality have also been proposed by Geman and Geman (1984), Hajek (1988), and Siarry (1997). These however may take too long for many practical problems (Cohn and Fielding, 1999). The wealth of practical experience with the faster t schedule used here indicates that the solutions found should be *good* local optimal ones. In practical terms: good approximate solutions are a compromise between relatively good solutions in an amount of time significantly smaller than the one necessary to guarantee the very good quality solutions provided (in theory) by slower schedules. In practice during the optimization procedure the program will have to call the kriging routine in all iterations to compute a new kriging variance. When the number of grid nodes is very large this computation is the bottleneck in computing times. By construction SA is essentially a sequential algorithm difficult to parallelize. This means that significant reductions in computation times may be more easily obtained by parallelizing the kriging matrix. Our results, however, were obtained using the sequential procedure. We consider here that the N central points of the model cells correspond to locations where it is possible to install a monitoring well, and for which there is previous information about the "real value" at that location. This "real value" is obtained by solving the advection-dispersion equation for mass transport. Hence, by selecting n of these data points ($n < N$) and using them to obtain estimates at the N points, it is possible to determine both the estimation error (difference between the estimate and the "real value"), and the mean kriging variance (Equation (6)).

Objective function

Our objective was to study the influence of uncertainty of the sources (their position and amounts released into groundwater) in the quality and spatial configuration of monitoring networks. The uncertainty in the sources was modeled by i) making several equally probable leakage scenarios (their number being identified by k, as determined by Equation (3)), ii) estimating the concentrations at the N data points for each of the k scenarios; iii) make the SA algorithm generate a solution with a set of n stations (X in the pseudo-code), evaluating the objective function, and proceeding to a next solution, or stop, and presenting the final solution. The objective function proposed here includes two terms: i) one for minimizing the mean estimation variance; ii) one for minimizing the mean absolute estimation errors between the kriging estimates with all N data points and those obtained with the n samples, and between all k scenarios. During optimization, kriging estimates are calculated with the variogram model computed on the fiftieth percentile (p_{50}) over all k scenarios – at each N points there will be k data values, the p_{50} value is chosen to calculate the variogram. This simplification is necessary to speed-up the computation of the objective function by eliminating the need to compute all k estimates on all optimization iterations. The first term of the objective function is calculated by Equation (6); the second term is the mean absolute estimation error (Ψ) between all k scenarios and the kriging estimate, C^*, obtained with the sample of n stations:

$$\psi = \frac{1}{k \cdot n} \sum_{i=1}^{k} \sum_{j=1}^{n} \left| C(i,j) - C^*(j) \right| \qquad (7)$$

The unconstrained objective function is:

$$\min \frac{1}{a}\sigma_E^2 + \frac{1}{b}\psi \qquad (8)$$

The constants a and b are normalizing parameters that correspond, respectively, to the data variance and maximum Ψ (obtained by making some prior SA runs with a very high initial temperature), intended to make the maximum value of the objective function to be close to two. This will make the relative contributions of the two terms similar, and makes easier the setting of the annealing parameters (essentially the initial temperature) because the maximum value of the objective function will remain below the value 2.0 whatever the values of k, N and n.

The proposed objective function includes a measure of the estimation accuracy, in the form of the estimation variance, and a measure of precision, in the form of Ψ. The advantage of including the latter term is that it adds information about how close the estimates, C^*, are from the k "real values". This information will allow the inclusion of stations in the final monitoring network that are more sensitive to the variability introduced by the uncertainty about the sources: the set of stations that minimize Ψ will have a configuration best adapted to detect contamination plumes even when these correspond to less probable contamination events (less frequent location of leakage, and/or less frequent amount leaked). Each time the kriging routine is called, n data points will be available for the routine to estimate the values at the N points (their estimated value and corresponding kriging variance). The optimization algorithm feeds the kriging routine with different spatial distributions of the n data points (solution), uses the estimated values to compute the objective function (Equation (8)), and makes the change in the solution according to the Metropolis criterion. New solutions are fed to the kriging routine until the SA algorithm reaches

any of the stopping criteria. The algorithm, as implemented, does not allow the direct determination of the best number of stations, *n*. This has to be evaluated iteratively by changing the value of *n* and optimizing again. Usually, as more stations are added, the more accurate the estimates, though marginal gains in accuracy tend to decrease for high n values (Nunes et al., 2003).

A specific FORTRAN 95 code was developed, OPTIVAR, that includes the kriging routine, simulated annealing and the modules to pre- and post-process data from MOFLOW and MT3D codes.

APPLICATION EXAMPLE

To test the method a hypothetical case study was created: i) porous unconfined aquifer; ii) conservative solute; iii) industrial area with spatially variable leakage probabilities and leaked quantities. The case study area consists in a region between two water bodies, one to the east and another to the west, distancing 1400 m. The water level in both water bodies is considered constant, and equal to 12 m to the former, and to 19 m to the latter, modeled as constant head boundaries (black borders in Figure 1). Some parts of the boundaries are impervious, corresponding to very low permeability rocks, modeled as inactive boundaries (grey boundaries in Figure 1). The aquifer has a constant thickness of 20 m, modeled as single layer. Contaminant enters the aquifer through the top, by leakage from an industrial area with 110 m E-W x 220 m N-S, modeled as contaminated recharge (white rectangle in Figure 1). The model assumes constant source concentration, a negligible volume of leachate relative to groundwater flow, and the leachate completely mixes over the entire thickness of the aquifer beneath the plume source. The continuous mass flux (g/m^2.d) at each cell was computed by multiplying the effective emission by a constant recharge value of 0.001 m^3/m^2.d. Simulation was made for 7300 days, corresponding to the time necessary for a significant concentration of solute to reach the eastern water body. Simulation was made in steady-state conditions. More domain and aquifer parameters are presented in Table 1.

The industrial area has several activities and/or infrastructures (pipelines, chemicals deposits, and industrial processes) with different probabilities of a leak (dependent on the type of operation, type and age of the equipment, maintenance, etc.). Probabilities associated with a leak are assumed essentially age-dependent, and are therefore distributed in space according to the temporal expansion of the plant in space (Figure 2b)). The amounts released are considered dependent on 14 types of activity, as shown in Figure 2a). Table 2 presents the parameters necessary to obtain the leakage estimates. Values, though in accordance with reality, are fictitious.

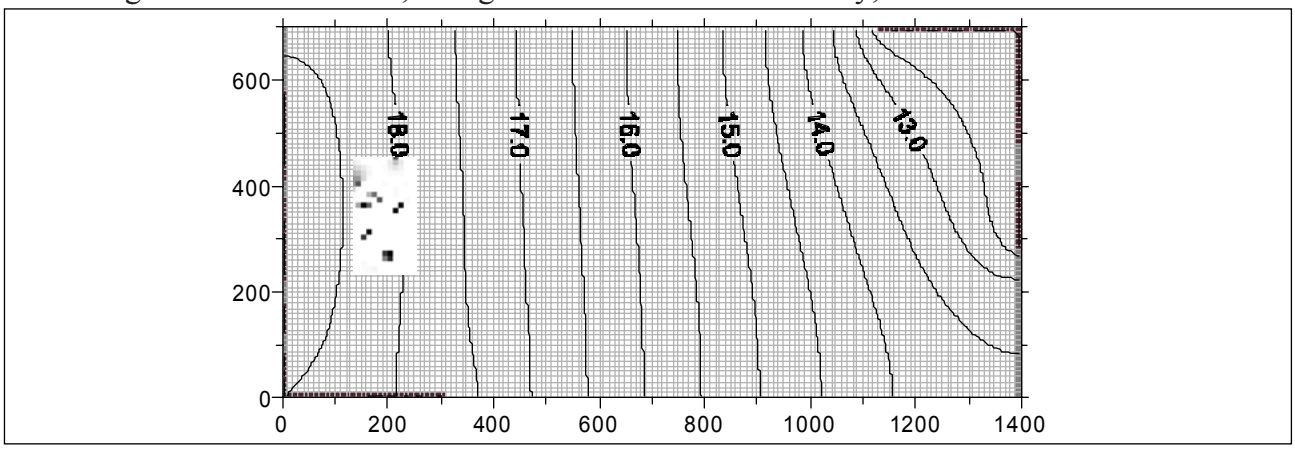

Figure 1. Model domain. Lines show piezometric heads (m). Industrial area is also shown - gray cells indicate different leachate concentrations.

Table 1. Model domain and aquifer parameters.

Domain	Mesh size	K (isotropic)	Effective porosity	Longitudinal dispersivity	Transverse horizontal dispersivity	Transverse vertical dispersivity
(m)	(m)	(m/d)	-	(m)	(m)	(m)
1400 E-W x 700 N-S	10 x 10	10	0.3	10	3	3

The computation of k was made on the logarithms of concentration to keep variance within reasonable intervals and because subsequent computations used log transformations of concentrations. After setting the values of $z_{a/2}$=0.80, d=0.25 and P=242 (number of grid cells inside the industrial area) in Equation (3) – i.e., accept a 25% error around the mean value for a two-sided confidence level of 0.2 -, the stochastic generation of leaked concentrations inside the industrial area was repeated for 30 times to obtain a mean value for k (being the *effective emission* generation algorithm a stochastic one (recall that in a given cell both the probability of being leaking and the amount leaked change each time a p value is taken), the value of s_e^2 is different each time it is calculated, within a limited range, and hence so is the value of k.) The resulting k value was 20 (rounded to the closest integer). The following annealing parameters were used: t_1= 1.0 or 2.0; η=0.9 or 0.95; *max_iterations*=5000; *max_best*=500 or 1000. The search for solutions

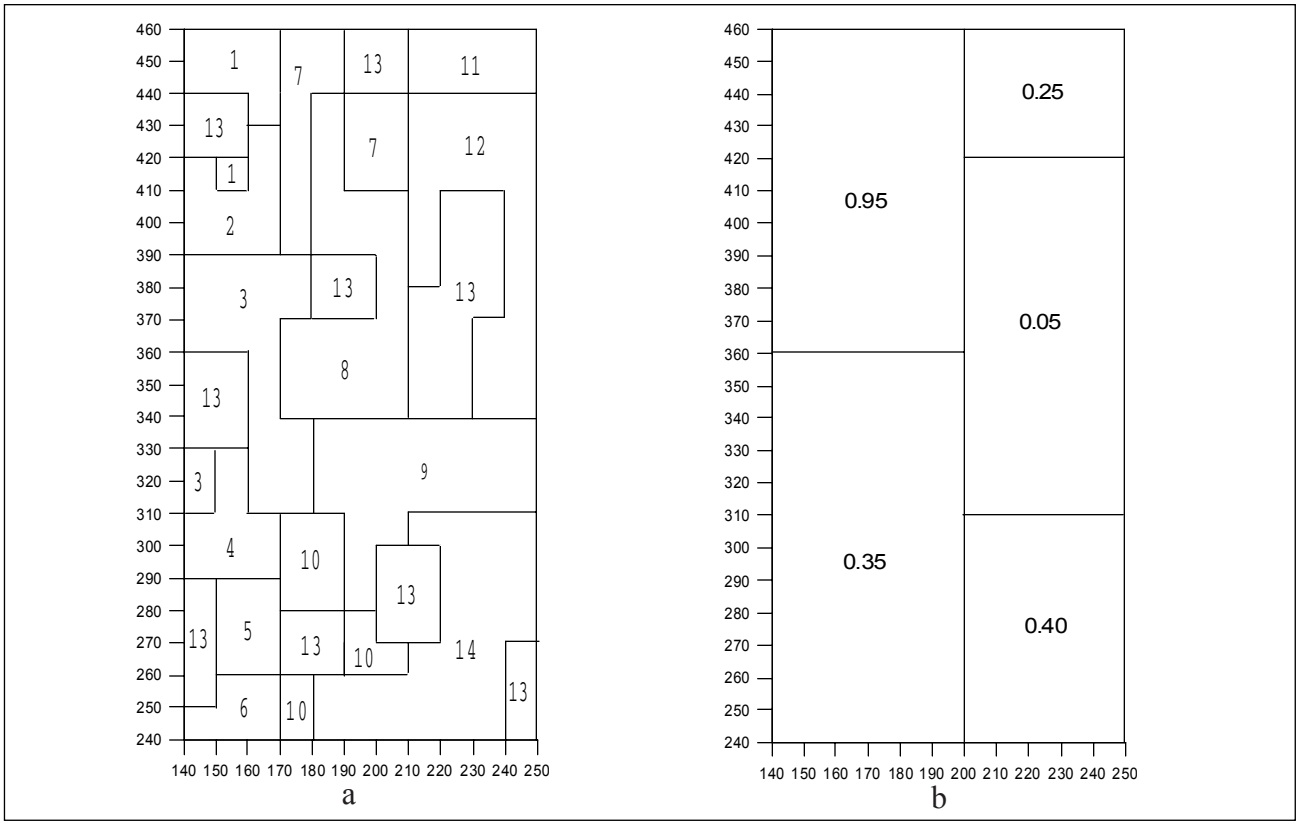

Figure 2. Industrial area: a) 14 sub-areas inside the industrial area; b) leakage probabilities.

Table 2. Parameters for the estimation of emissions inside the industrial area.

	Sub-area, i													
Parameter	1	2	3	4	5	6	7	8	9	10	11	12	13	14
m_i (g/m^3)	1500	1200	50	1	10000	40	80	200	700	1100	900	300	20000	1000
δ_i	0.02	0.080	0.5	0.01	0.05	0.3	0.8	0.6	0.7	0.075	0.9	0.005	0.005	0.15
p_i	See Figure 2													

stopped when after three consecutive temperature decreases the average OF did not change. All runs were made in a personal computer equipped with an Intel Pentium(R)M processor (2000 GHz), 2.00 GB of RAM (797 MHz).

RESULTS AND CONCLUSIONS

Twenty (k) mass-transport simulations were made with MT3D for 7300 days. Figure 3 shows one example of a concentration field, where the high concentration variability near the sources is very clear: monitoring wells wrongly located may easily skip detection, or indicate a much lower/higher average concentration.

The following n values were iteratively tested: 10, 15, 20, 25, 30, 40, 50, 60, 70, 80 and 90. For each of these n values, at least three annealing runs were made with three different initial solutions to test the algorithm for robustness (a total of 9 runs for each n). Adjustments to the annealing parameters were made and the runs repeated whenever, with the same set of annealing parameters, the values of the final solutions of optimization differed more than 5%. Results from the optimization runs are presented in Table 3 and Figure 4. In the former is also presented: i) the solution space size; ii) the value of the OF averaged over the 9 SA runs; iii) corresponding standard deviation; iv) the value of the best final solution; and v) the averaged optimization run time. The values of the standard deviation of the mean OF are very low for all tested n, which is a consequence of the criterion for accepting final solutions; another consequence is the proximity of the best OF value to that of the mean. One interesting aspect is the growth in running time, which does not

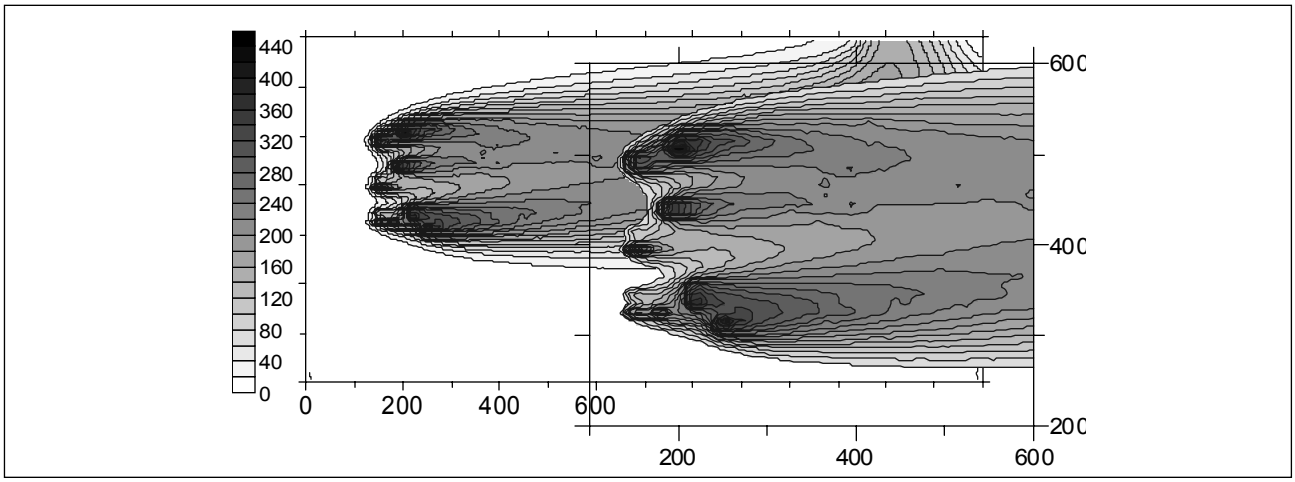

Figure 3. Example of a solute concentration plume after 7300 days (g/m3). Overlapping figure is a zoom in on the emission area.

Table 3. Optimization results.

n	Solution space size Log(combinations)	Average of OF	St. dev. of OF	Best OF	Average run time (s)
10	19.26	0.8212	0.0017	0.8196	29931
15	26.56	0.8000	0.0041	0.7942	8806
20	33.13	0.7926	0.0062	0.7840	5025
25	39.13	0.7779	0.0062	0.7779	37460
30	44.67	0.7695	0.0017	0.7675	5189
40	54.64	0.7636	0.0019	0.7629	5758
50	63.41	0.7613	0.0003	0.7609	8176
60	71.17	0.7670	0.0005	0.7590	22018
70	78.09	0.7662	0.0005	0.7658	39895
80	84.24	0.7668	0.0005	0.7668	82114
90	89.72	0.7636	0.0004	0.7632	77065

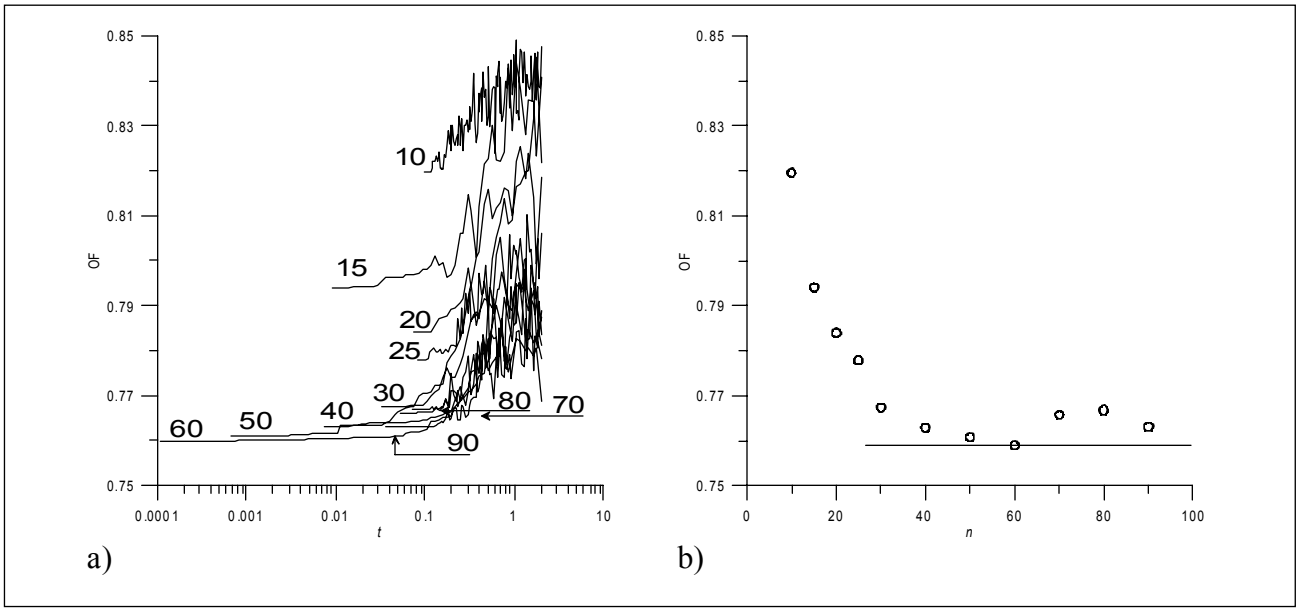

Figure 4. a) SA convergence curves for the runs with the best OF; b) tradeoff between number of stations in the monitoring network and OF value.

follow the relative increase in the solution space (number of combinations): the time necessary to solve for $n = 80$ is only one order of magnitude higher than for $n = 15$, despite the increase of more than 57 orders of magnitude in the solution space. This may be the consequence of a fast cooling schedule (combination of both the cooling rate, η, and the dimension of the Markov chain at each temperature) considered as necessary to obtain good solutions in a reasonable amount of time (the runs for $n = 80$ already took almost one day each). Higher cooling rates (e.g., 0.975) were tested, but resulted in only marginally better (<5%) OF values; increasing the dimension of the Markov chain up to 5 times also did not improve the value of the OF. Important gains are expected with much higher cooling rates and/or increases in the dimension of the Markov chain higher than one order of magnitude. Both of these changes would, however, shoot the running times to values in the order of several days or weeks. We believe that the cooling schedule used here is the best suited to the problem, by keeping running times within reasonable times, while generating solutions of very good quality.

Figure 4 shows the SA convergence curves for the best final solutions for each of the n values, and the value of OF for different number of stations in the monitoring network. Common features to all convergence curves are: i) the evolution from high OF values to lower ones; ii) higher variability at higher temperatures; iii) in general, as more stations are added, the lower the OF value, up to a certain point. The first two features result from the algorithm itself by allowing more moves to worst solutions at higher temperatures, and by slowly reducing the probability of this happening as temperature decreases. The latter feature is case-specific and is a result from the OF equation: the spatial accuracy term causes the OF to decrease as more stations are added; however the second term will penalize stations with higher estimation error, and therefore as more stations are added, more stations with high errors will have to be included (though some of the effect may be dampened by the higher estimation precision of kriging). This may explain the reduction in the marginal OF gains as more stations are added, and also the increase observed for $n > 60$ (Figure 4b). Considering the stabilization in marginal OF gains after $n = 60$, there seems to be little interest in adding more stations beyond this point.

After having obtained the ideal n value, and the optimized spatial distribution of stations (see Figure 5), there is still the question of whether a more empirical approach would have given better

results. By empirical we understand that a decision maker will preferably allocate the stations in places where he expects higher concentrations, or use a traditional sampling design, of which the stratified sampling is one of the most widely used. The first approach will increase the probability of detecting the highest values when the network is very dense and concentrated near the origin, but will most probably leave undetected areas with lower concentrations. Moreover, it makes the estimate of the affected area and water volume very difficult. The latter approach usually allows better representation of concentration fields, but the precision depends on the density of the sampling. Both these methods will, however, disregard any complementary information. We make below a comparison between the optimized networks and two of such empirical network designs: i) empirical clustered, where stations are located near the source in a regular grid; ii) empirical stratified, where stations are located in a regular grid twice as narrow near the source as further westward. Figure 5 shows the proposed monitoring networks for $n = 60$ (the other n are not shown due to space limitations); Table 4 presents some statistics obtained for a sample size of n: i) estimated average concentration (*eac*); i) variance of estimated average concentration (as before) (*veac*); iii) estimated mean kriging variance (*mekv*), i.e., the mean kriging variance computed for all N data points with the sample and the variogram model used before (on the p_{50} of concentrations); iv) mean absolute estimation error (*maee*), computed between the values estimated by kriging with

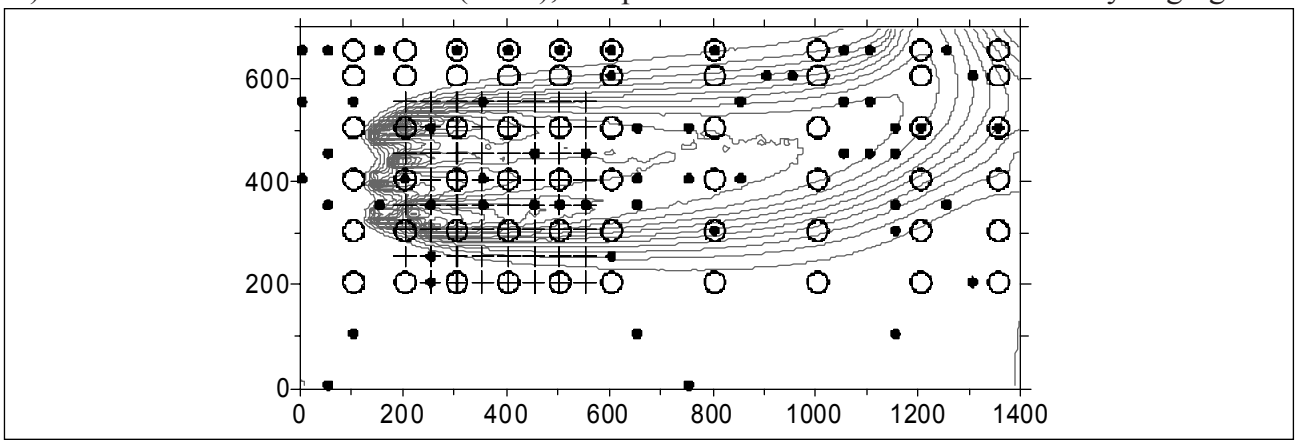

Figure 5. Resulting n=60 monitoring networks: •: Optimized network; o: empirical stratified; +: empirical clustered.

Table 4. Statistics for optimized and empirical networks (see text). Values as Log (concentration).

n	Optimized networks				Empirical stratified				Empirical clustered			
	eac	veac	emkv	maee	eac	veac	emkv	maee	eac	veac	emkv	maee
10	-0.864	1.782	4.705	1.269	0.907	0.406	6.382	2.733	1.039	0.827	5.440	2.858
15	-0.788	1.841	3.949	1.238	0.348	0.731	5.675	2.219	0.534	0.641	5.631	2.546
20	-0.626	2.217	3.684	1.285	0.308	0.822	5.606	2.161	0.742	1.000	5.320	2.667
25	-0.975	2.478	3.621	1.120	0.348	0.979	5.271	2.105	0.917	1.222	5.134	2.800
30	-0.744	2.943	3.340	1.071	0.114	1.496	5.025	1.859	0.919	1.272	5.116	2.808
40	-0.852	2.916	3.221	0.991	-0.024	1.705	4.906	1.691	0.787	1.565	5.359	2.748
50	-0.885	3.074	3.163	0.917	-0.119	3.068	4.339	1.522	0.083	2.946	4.831	1.709
60	-0.905	3.120	3.145	0.891	-0.198	3.225	4.321	1.445	1.005	1.326	5.971	2.806
70	-0.904	3.032	3.289	0.940	-0.488	2.474	3.956	1.167	1.009	1.320	5.911	2.809
80	-0.874	2.958	3.318	0.982	-0.518	2.537	3.971	1.139	0.544	2.265	5.675	2.931
90	-0.917	3.136	3.273	0.917	-0.520	2.534	3.972	1.136	0.430	1.861	5.417	2.817
R	-1.617	5.662										

Eac: Estimated average concentration (g/m^3); *veac*: Variance of estimated average concentration $(g/m^3)^2$; *emkv*: Estimated mean kriging variance $(g/m^3)^2$; *maee*: Mean absolute estimation error between the original field and the field estimated with *n* stations (g/m^3) – is a measure similar to the one used in the objective function, but calculated with only two fields.

the sample, and the original p_{50} concentration data, for all N data points. These statistics will give some insight as to, respectively: i) the bias introduced in the (measured by the network) mean receptor concentration estimated with the sample; ii) idem for the variance; iii) bias in the accuracy of estimation – incorrect position of monitoring stations may lead to highly inaccurate estimation of spatial variability of receptor concentrations; iv) bias in the estimation of mean values over the field – incorrect estimation of contaminated volumes and areas. Best spatial distributions have values of the first two statistics closest to the reference field, R (obtained with all data points); and values of the latter two closest to zero.

The statistics are shown in Table 4 where the best values are underlined. It is evident the much better performance of the optimized design over the empirical, with the only exception of $n = 60$, for which the *veac* is closer to the reference in the stratified design. This may be explained by the fact that the more regular design captured best the data variability, i.e., the samples collected best represented the "real" data variability. However, this design was very poor with regard to all the other statistics, making it a second choice over the optimized design. The results shown graphically in Figure 5 report only to the case of $n = 60$, where the significantly different spatial distributions are clear. The same results were also observed for other values of n (not shown here for space limitations). Another interesting result is the convergence in the performance of the stratified method to the optimized one as n increases, unlike the clustered method (see Figure 6). This may indicate that stratified designs may work well when the number of stations is high to very high, but may never attain the performance of optimized methods. This conclusion shows that case-specific methods will work best (as they should).

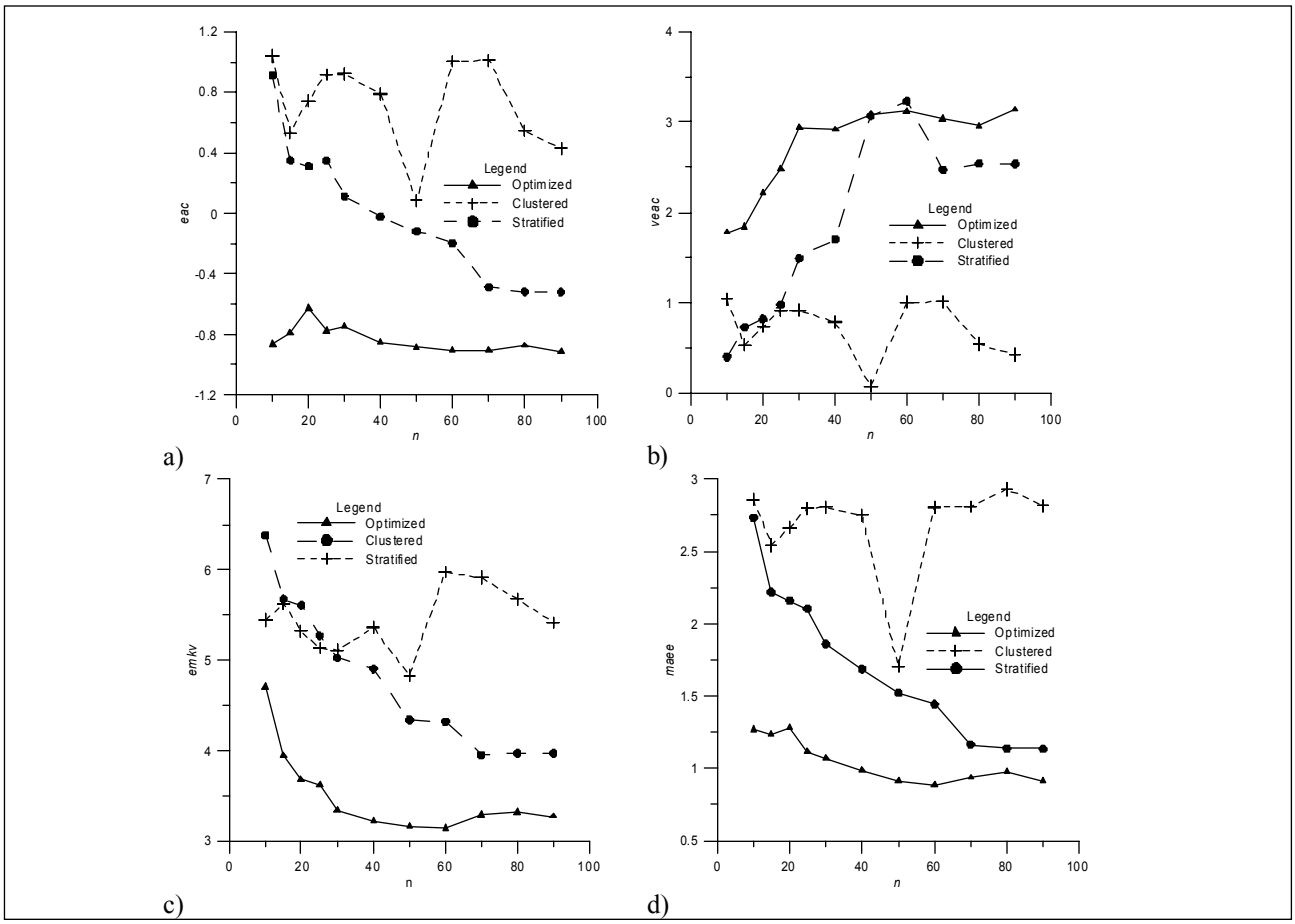

Figure 6. Comparison of methods for locating stations. a) *eac*; b) *veac*; c) *emkv*; d) *maee*.

ACKNOWLEDGMENTS

This work was supported by the Portuguese Foundation for Science and Technology (Fundação Nacional para a Ciência e a Tecnologia) under contract POCI/ECM/56263/2004. The author also acknowledge the reviewing made by Dr. Tibor Stigter from the Instituto Superior Técnico, Lisbon, and Dr. José Paulo Monteiro from the University of Algarve.

REFERENCES

Aarts, E. and Korst, J. 1990. Simulated Annealing and Boltzmann Machines. New York: John Wiley and Sons.

Abt, M. Welch, W.J. and Sacks, J. 1999. Design and analysis for modeling and predicting spatial contamination. Mathematical Geology, Vol. 31 (1), pp. 1-22.

ASCE 2003. Long-Term Groundwater Monitoring - the State of the Art. USA: American Society of Civil Engineers.

Atmadja, J. and Bagtzoglou, A.C. 2001. State of the art report on mathematical methods for groundwater pollution source identification. Environmental Forensics, Vol. 2, pp. 205-214.

Bear, J. 1972. Some Experiments in Dispersion. Journal of Geophysical. Research, Vol. 66, pp. 2455-2467.

Belke, J.C. 2000. Chemical Accident Risks in U. S. Industry - a Preliminary Analysis of Accident Risk Data From U. S. Hazardous Chemical Facilities (Washington, D. C., USA: United States Environmental Protection Agency - Chemical Emergency Preparedness and Prevention Office).

Cerny, V. 1985. Thermodynamical approach to the traveling salesman problem: an efficient simulation algorithm. Journal of Optimisation Theory and Applications, Vol. 45, pp. 41-51.

Cohn, H. and Fielding, M. 1999. Simulated annealing: searching for an optimal temperature schedule. SIAM Journal on Optimization, Vol. 9 (3), pp. 779-802.

EEA 1999. Chapter 3.6. Soil Degradation Environment in the European Union at the Turn of the Century - State of Environment Report No 1/1999 European Environment Agency (Copenhagen, Denmark).

Erickson, M. 1997. Analytical Chemistry of PCBs. Lewis Publishers, CRC Press.

Geman, S. and Geman, D. 1984. Stochastic Relaxation, Gibbs Distributions and the Bayesian Restoration of Images. IEEE Transaction on Pattern Analysis and Machine Intelligence, Vol. PAMI-6 (6), pp. 721-741.

Hajek, B. 1988. Cooling schedules for optimal annealing. Mathematics of Operations Research, Vol. 13 (2), pp. 311-329.

Hudak, P.F. 2005. Sensitivity of Groundwater Monitoring Networks to Contaminant Source Width for Various Seepage Velocities. Water Resources Research, Vol. 41 (8), w08501.1-w08501.4

Journel, A. and Huijbregts, Ch. 1978. Mining Geostatistics. New York, U.S.A.: Academic Press.

Kaunas, J.R. and Haimes, Y.Y. 1985. Risk management of groundwater contamination in a multiobjective framework. Water Resources Research, Vol. 21 (11), pp. 1721-1730.

Kirkpatrick, S., Gellat, Jr. C.D. and Vecchi, M.P. 1983. Optimization by simulated annealing. Science, Vol. 220 (4598), pp. 671-680.

Laarhoven, P.J.M. and Aarts, E. 1987. Simulated Annealing: Theory and Applications. Dordrecht: Reidel.

Lydell, B.O.Y. 2000. Pipe failure probability - the Thomas paper revisited. Reliability Engineering and System Safety, Vol. 68, pp. 207-217.

Massmann, J. and Freeze, R.A. 1987a. Groundwater contamination from waste management sites: the interaction between risk-based engineering design and regulatory policy, 1. Methodology. Water Resources Research, Vol. 23 (2), pp. 351-367.

Massmann, J. and Freeze, R.A. 1987b. Groundwater contamination from waste management sites: the interaction between risk-based engineering design and regulatory policy, 2. Results. Water Resources Research, Vol. 23 (2), pp. 368-380.

McDonald, M.G. and Harbaugh, A.W. 1988. A Modular Three-Dimensional Finite-Difference Ground-Water Flow Model, Book 6, Chapt. 6 U.S. Geol. Surv. Techn. Water-Resour. Inv. (USA: United States Geological Survey).

Mercer, J.W. and Cohen, R.M. 1990. A review of immiscible fluids in the subsurface: Properties, models, characterization, and remediation. Journal of Contaminant Hydrology, Vol. 6 (2), pp. 107-163.

Metropolis, N., Rosenbluth, A.W., Rosenbluth, M.N., Teller, A.H. and Teller, E. (1953). Equation of state calculations by fast computing machines. The Journal of Chemical Physics, Vol. 21 (6), pp. 1087-1092.

Meyer, P. D., Neuman, S.P. and Cantrell, K.J. 2004. Combined Estimation of Hydrogeologic Conceptual Model and Parameter Uncertainty, NUREG/CR-6843 Technical Report prepared for USNRC, NUREG/CR-6843 U.S. Nuclear Regulatory Commission (U.S:A.: U.S. Nuclear Regulatory Commission).

Meyer, P.D., Valocchi, A.J. and Eheart, J.W. 1994. Monitoring network design to provide initial detection of groundwater contamination. Water Resources Research, Vol. 30 (9), pp. 2647-2659.

Morrison, R.D. 2000a. Critical review of environmental forensic techniques: Part I. Environmental Forensics, Vol. 1, pp. 157-173.

Morrison, R.D. 2000b. Critical review of environmental forensic techniques: Part II. Environmental Forensics, Vol. 1, pp. 175-195.

Newell, J.C., Acree, S.D. and Randall, R.R. 1995. Ground Water Issue - Light Nonaqueous Phase Liquids Ground Water Issue - Light Nonaqueous Phase Liquids, EPA/540/S-95/500 United States Environmental Protection Agency (Oklahoma, USA: EPA).

Nunes, L.M., Caeiro, S., Cunha, M.C. and Ribeiro, L. (2003). Optimal estuarine sediment monitoring network design with simulated annealing. Journal of Environmental Management, 78 (3), 294-304.

Nunes, L.M., Paralta, E., Cunha, M.C.C. and Ribeiro, L. 2004. Groundwater nitrate monitoring network optimization with missing data. Water Resources Research, Vol. 40 (2), pp. 1-18.

Ramamoorthy, S. and Ramamoorthy, S. 1997. Chlorinated Organic Compounds in the Environment; Regulatory and Monitoring Assessment. Boca Raton, FL: Lewis Publishers, CRC Press.

Reinelt, L.E., Horner, R.R. and Mar, B.W. 1988. Nonpoint source pollution monitoring program design. Journal of Water Resources Planning and Management - ASCE, Vol. 114 (3), pp. 335-352.

Scheibe, T.D. and Lettenmaier, D.P. 1989. Risk-based selection of monitoring wells for assessing agricultural chemical contamination of ground water. Ground Water, Vol. 11 (4), pp. 98-108.

Siarry, P. 1997. Enhanced simulated annealing for globally minimizing functions of many-continuous variables. ACM Transactions on Mathematical Software, Vol. 23 (2), pp. 209-228.

Small, M.J. 1997. Groundwater detection monitoring using combined information from multiple constituents. Water Resources Research, Vol. 33 (5), pp. 957-969.

Storck, P., Eheart, J.W. and Valocchi, A.J. 1997. A method for the optimal location of monitoring wells for detection of groundwater contamination in three-dimensional heterogenous aquifers. Water Resources Research , Vol. 33 (9), pp. 2081-2088 .

Stout, S.A., Uhler, A.D., Naymic, T.G. and McCarthy, K.J. 1998. Environmental forensics unraveling site liability. Environmental Science and Technology, Vol. 32 (11), pp. 260A-264A.

Sun, A.Y., Painter, S.L. and Wittmeyer, G.W. 2006. A Robust Approach for Iterative Contaminant Source Location and Release History Recovery. Journal of Contaminant Hydrology, Vol. 88 (3-4), pp. 181-196.

Sun, N.-Z. 1994. Inverse Problems in Groundwater Modeling. The Netherlands: Kluwer Publishers.

Thomas, H.M. 1981. Pipe and vessel failure probability. Reliability Engineering, Vol. 2, pp. 83-124.

USEPA 2006 Federal Underground Storage Tanks Program - Corrective action measures archive [Web Page] (Available at http://www.epa.gov/oust/cat/camarchv.html, accessed 2007).

Widory, D., Kloppmann, W., Chery, L., Bonnin, J., Rochidi, H. and Guinamant, J.-L. 2004. Nitrate in groundwater: an isotopic multi-tracer approach. Journal of Contaminant Hydrology, Vol. 72, pp. 165-188.

Woldt, W. and Bogardi, I. 1992. Ground water monitoring network design using multiple criteria decision making and geostatistics . Water Resources Bulletin, Vol. 28 (1), pp. 45-62.

Zemo, D.A., Bruya, J.E. and Graf, T.E. 1995. The application of petroleum hydrocarbon fingerprinting characterization in site investigation and remediation. Ground Water Monitoring and Remediation, Vol. 15 (2), pp. 147-156.

Zheng, C. 1990. MT3D: A Modular Three-Dimensional Transport Model for Simulation of Advection, Dispersion and Chemical Reactions of Contaminants in Ground Water Systems S. S. Papadopulos and Assoc. R Md (USA).

ADDRESS FOR CORRESPONDENCE
Luís Miguel Nunes
Faculty of Sciences and Technology
University of Algarve
Faro, Portugal

Email: lnunes@ualg.pt